Thrust Augmentation by After-Burning in a Scramjet Nozzle

M.J. Candon, H. Ogawa and G.E. Dorrington

School of Aerospace, Mechanical and Manufacturing Engineering
RMIT University, PO Box 71, Bundoora, VIC 3083, Australia

Abstract

A numerical study of scramjet after-burning through the injection of liquid oxygen into the nozzle is conducted. A maximum thrust augmentation of 300% is found. An understanding of the thrust augmentation phenomenon is provided in the form of a force contribution breakdown, analysis of the nozzle flowfields and finally the analysis of the surface pressure and shear stress distributions acting upon the nozzle wall.

Introduction

Scramjet (supersonic combustion ramjet) propulsion eliminates the need to carry an oxidiser and offers higher specific impulse than conventional rocket engines. A scramjet cycle demonstrated in Figure 1 involves an intake of hypersonic air which is compressed to high pressure and temperature, fuel is then injected and combusted supersonically in the combustion chamber. The exhaust gas is then expanded through the nozzle, resulting in net thrust.
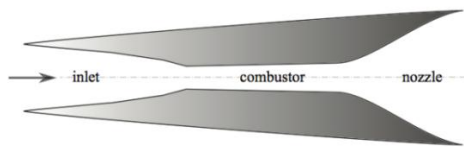

Figure 1. Schematic of an axisymmetric scramjet with flow direction [10].

The expanding exhaust gas comprises of a significant proportion of unburned hydrogen which under ideal conditions can be combusted via the injection of liquid oxygen directly into the unburned hydrogen stream, i.e. by introducing after-burning. This has the potential to significantly increase the thrust produced by the nozzle whilst also maintaining an ideal nozzle expansion ratio ($p_{exit} = p_{atm}$) by decreasing the injection pressure of liquid oxygen as flight altitude increases. A schematic of the after-burning scheme is presented in Figure 2.
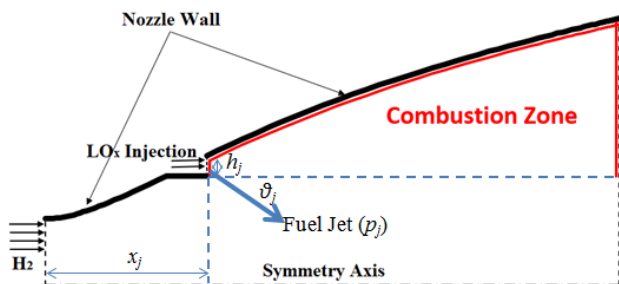

Figure 2. Schematic of the scramjet after-burning scheme, injection parameters highlighted in blue (injector not to scale).

There are several critical factors that must be considered with such an after-burning scheme including mixing of reactants, ignition and completion of combustion. The phenomenon that are associated with supersonic combustion also introduce several difficulties into the supersonic flowfield such as turbulent mixing, shock interaction and heat release [8]. The ramp-injector configuration shown in Figure 2 allows efficient mixing with near streamwise injection, this minimises losses due to low pressure gradients downstream of shocks induced by an injection angle. The ramp also provides a region for flame holding and flame stabilisation through the buildup of a radical pool [4]. However the benefits of a ramp injector remain provided that the geometry does not result in too severe a local flow disturbance as this may result in pressure losses as well as more demanding wall cooling requirements [5].

This paper builds upon research conducted by Ogawa and Boyce [10] who considered the design optimisation of an axisymmetric scramjet nozzle for the discontinued SCRAMSPACE project conducted by the University of Queensland [1], the optimised geometry acts as the baseline and validation geometry for the present study. The optimisation of the nozzle contour was based upon nozzle inflow conditions that were obtained from a separate CFD simulation in which the scramjet intake and combustor were included. The nozzle inflow therefore contained reacted gases and for the present study these nozzle inflow conditions remain unaltered.

The optimised geometry obtained by Ogawa and Boyce [10] is adapted by including the injection of liquid oxygen via the ramp configuration. The influence of several parameters on thrust augmentation is investigated including the injection pressure, streamwise injection position and injection angle. The streamwise injection position influences the mixing and combustion time significantly. Further, the position of the injector should be such that temperatures and pressures of the crossflow are sufficiently high promoting sufficient fast combustion [8]. As the injection angle increases, enhanced penetration, mixing and combustion occurs. However, higher injection angles lead to intensified levels of interaction between the injected oxygen and the crossflow, causing upstream and downstream wall flow separation and increased wall static temperatures. The injection pressure influences the penetration levels of the fuel jet such that higher pressure leads to higher levels of penetration and allows for enhanced mixing and combustion. The momentum produced by the injected oxygen also directly influences the augmentation of thrust and higher injection pressures yield a greater momentum increase. The extremely complex nature of the scramjet nozzle flowfield means that it is imperative to optimise the aforementioned injection parameters in order to promote maximum thrust augmentation.

Methods

Conditions and Configurations

The present study considers an axisymmetric scramjet operating at Mach 8 at an altitude of 27 km with a freestream static pressure and temperature of 1847 Pa and 223.7 K, respectively, with a constant dynamic pressure trajectory of 82.5 kPa. A Reynolds number of 3.53×10^5 is used based on an inlet capture radius of 0.075 m. The nozzle inflow profiles obtained from

Ogawa and Boyce [10] included pressure, temperature, Mach number, turbulence and species profiles as presented in Figure 3.
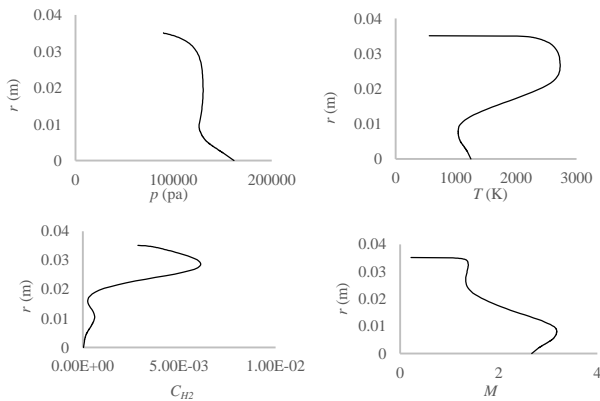

Figure 3. Nozzle inflow profiles for pressure (top left), temperature (top right), hydrogen mass fraction (bottom left) and Mach number (bottom right).

The optimisation conducted by Ogawa and Boyce [10] considered the nozzle entrance position in the axial direction and the nozzle radius fixed at 0.808 m and 0.0351 m respectively which remains unaltered. For the present parametric study, the injection pressure p_j, injection angle θ_j and streamwise injection position x_j as a fraction of the nozzle length l_n are modified according to Table 1. The injector height h_j is fixed at 2 mm.

Distance from Nozzle Throat x_j (fraction of l_n)	Injection Angle θ_j (°)	Injection Total Pressure p_{0j} (bar)
0.125	0	5
0.25	15	10
0.375	30	15
0.5	45	20
-	60	25

Table 1. Parameters to be implemented for the present study.

Computational Fluid Dynamics

The flowfields for the scramjet nozzle are computed using the commercial code ANSYS Fluent. Both the nozzle and injector inflows are assumed to be fully turbulent and modelled with the two-equation SST k-ω RANS model. The Evans and Schexnayder model is used to represent both the reacting exhaust flow and the supersonic hydrogen-oxygen combustion resulting from the oxygen injection, with 12 species and 25 elementary reactions considered [6]. A two-dimensional structured computational mesh is generated via ANSYS Fluent Meshing, consisting of 32,350 cells, presented in Figure 4. The dimensionless wall distance y^+ ranges from 1.1 to 4.5 along the nozzle wall surface. This mesh resolution is selected based on a mesh refinement study. The fixed flow conditions of the injector consider sonic fuel injection (M_j=1) and a static temperature of T_j=250K. The body of the scramjet is considered to be comprised of isothermal cold walls at 300K, which is considered valid for impulse facility or short duration flight testing [10]. Pressure far-fields are imposed on all inlets and pressure outlets on all outlets.

A simulation incorporating the baseline geometry and nozzle inflow profiles as obtained from Ogawa and Boyce [10] is utilised for cross-validation purposes. Ogawa and Boyce [10] solved for the scramjet flowfields with the commercial CFD code CFD++ which is the code utilised in the Australian hypersonics community due to its high fidelity and validation against experimental results [10]. The cross-validation is conducted to ensure that the flowfields being solved through ANSYS are consistent with those solved in CFD++. A deviation in total axial force of 3.4% is obtained validating that the scramjet nozzle is accurately modeled by ANSYS. Further ANSYS appears to have captured a more detailed representation of the flowfield characteristics than CFD++, such as the pressure rise due to the shock impingements on the nozzle wall.
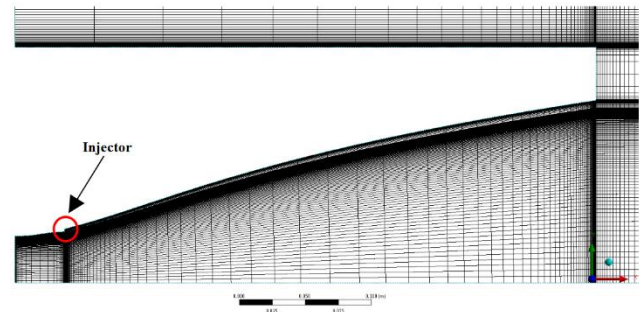

Figure 4. Enhanced view of the computational mesh (injector at $0.125 \times l_n$).

Results

Total Axial Force

The total axial force F_x acting on the nozzle is calculated including the contribution of viscous and inviscid forces acting on the nozzle and exterior walls. It is found that the total injection pressure is the dominating factor when considering the level of thrust augmentation that can be attained, such that higher injection pressures lead to higher levels of thrust augmentation. Table 2 presents the combination of parameters which are found to be optimum, inducing the highest total axial force in comparison to the baseline geometry. It is found that at $\theta_j = 30°$ the greatest level of thrust augmentation is obtained. For injection angles less than this sufficient penetration does not occur. For steeper injection angles, the losses incurred due to intensified levels of interaction between the fuel jet and the cross-flow, causing upstream and downstream flow separation, become too significant and surpass the enhanced levels of penetration. At $x_j = 0.375$ the fuel jet is able to obtain ideal levels of penetration, with the injector closer to the nozzle throat, sufficient penetration does not occur due to the high pressure of the crossflow. As the injector moves further downstream of the nozzle throat, the lower temperatures of the crossflow lead to insufficient combustion. The total axial forces that are obtained as the streamwise injection position and injection angle are varied for $p_{0j} = 25$ bar are presented in Figure 5.

Parameter	Optimum	Baseline
x_j (fraction of l_n)	0.375	-
θ_j (°)	30	-
p_{0j} (bar)	25	-
F_x (N)	2233	554

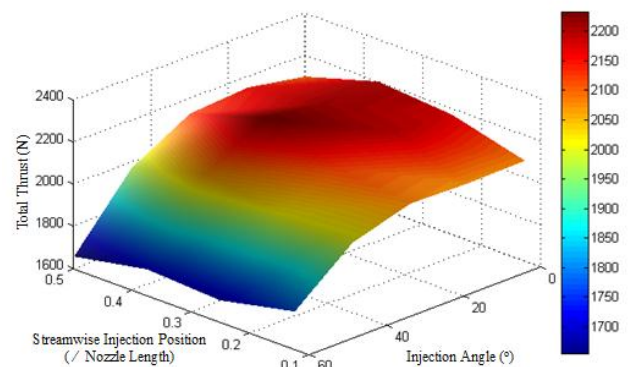Table 2. Parameters and total thrust for the optimum configuration.

Figure 5. Total axial force contour plot for an injection total pressure of 25 bar with respect to streamwise injection position and injection angle.

Force Breakdown

In order to determine the source of axial forces, Figures 6-8 present a breakdown of the inviscid, viscous and jet force contributions. The total axial force is significantly dominated by the inviscid force acting on the nozzle wall (thrust). There is also a significant contribution that can be attributed to the momentum increase caused by the fuel jet and a small contribution attributed to the inviscid force on the nozzle base. Whilst viscous (drag) forces on the nozzle and freestream wall are present, they are significantly outweighed by the inviscid forces. It should be noted that as the injection pressure increases, viscous forces on the nozzle wall increase and as the injection angle increases, viscous forces on the nozzle wall decrease. However, this occurrence is not significant enough to impact the overall thrust augmentation.

Figure 8 demonstrates the level of thrust augmentation that is produced for the optimum injection configuration as compared with the baseline geometry. It is apparent that a significant portion of the thrust augmentation is attributed to the momentum increase by the fuel jet, the energy required to achieve this momentum is likely to significantly counteract the net gain in thrust and thus it is likely that the net thrust is not as pronounced as indicated, quantifying and addressing this matter is a prospect for future work.
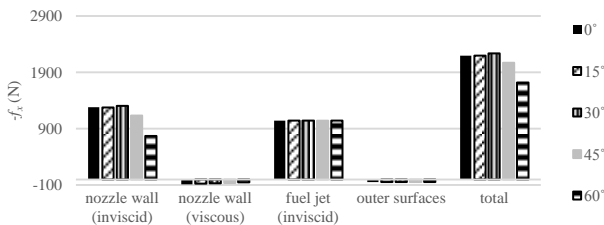

Figure 6. Force breakdown of axial force components ($x_j = 0.375$, $p_{0j} = 25$ bar) with injection angle variation.
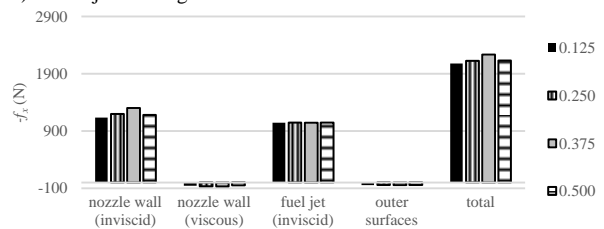

Figure 7. Force breakdown of axial force components ($\theta_j = 30°$, $p_{0j} = 25$ bar) with injection position variation.
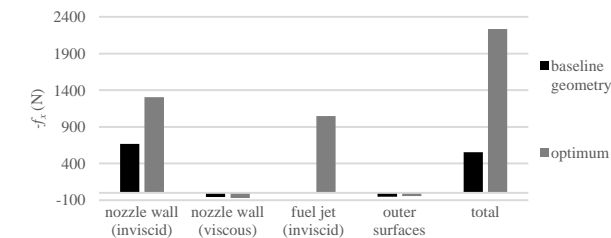

Figure 8. Comparison of force breakdown of axial force components between baseline and optimum cases.

Nozzle Flowfields

Flowfields for Mach number and hydrogen mass fraction are produced comparing the cases of baseline geometry and optimum injection configuration, as presented in Figures 9 and 10. Observation of Figure 9 indicates that the oxygen achieved substantial penetration into the crossflow, leading to combustion of the remaining hydrogen. However, with enhanced mixing the level of combustion is expected to amplify. Figure 10 indicates considerable effects of oxygen injection on the crossflow, where a prominent bow shock is formed due to interactions between the fuel jet and crossflow followed by expansion in the separated region downstream. Reflection of the fuel jet on the symmetry axis can be observed at approximately $x = 1$ m followed by an impingement on the nozzle wall between $x = 1.1$ and 1.2 m causing further expansion.

Whilst combustion is observed, the phenomenon is not as significant as expected. This is assumed to be attributed to inadequate mixing as well as little occurrence of ignition due to insufficient temperatures and pressures, as the injection position moves downstream of the nozzle throat. The axisymmetric nature of the problem makes a significant contribution to the current inadequate mixing. In order to enhance the mixing and combustion, the turbulence, reaction and diffusivity models shall be examined and revised.
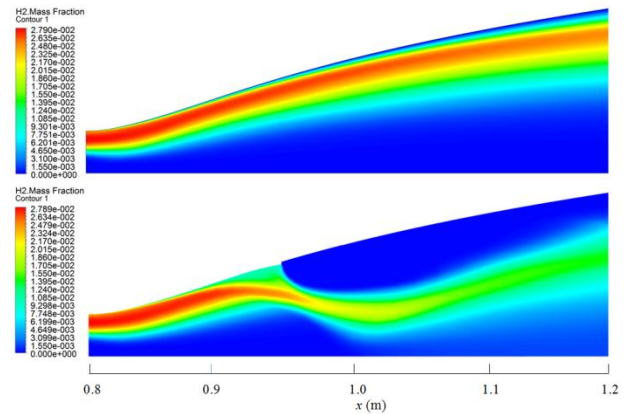

Figure 9. Hydrogen mass fraction distributions for baseline geometry (top) and optimum injection case (bottom).
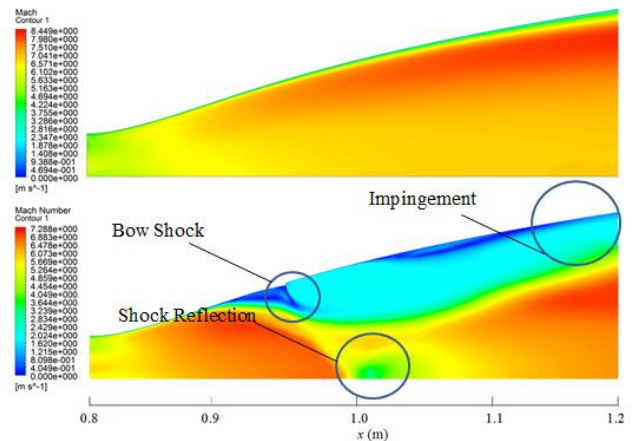

Figure 10. Mach number distributions for baseline geometry (top) and optimum injection case (bottom).

Surface Forces

The axial forces acting on the nozzle surface are attained by integrating the pressure and shear stresses acting upon the inner nozzle wall [10]. The surface pressure and shear stress distributions plotted in Figures 11 and 12 indicate that the introduction of the injector geometry, without fuel injection, leads to shock impingement occurring upstream of where the shock impingement occurs in the absence of the injector. Inspection of the case of optimum injection configuration indicates a significant increase in surface pressure in the region of the injection point and just upstream of the nozzle exit. The increase upstream of the nozzle exit can be attributed to the reflection of the fuel jet in the axisymmetric configuration; a total surface pressure increase of 2857 Pa is achieved. The shear stress distributions demonstrate similar behaviour and an increase of 70 Pa is found. The main source of thrust augmentation appears to

be occurring due to the extreme surface pressure increases that are observed in the injection region and at the nozzle exit. The increase in shear stress on the nozzle wall is not found to be significant as the increase in surface pressure is by far dominant.
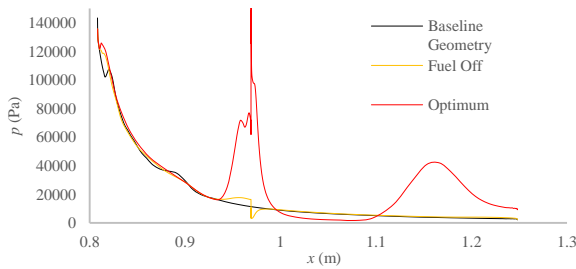
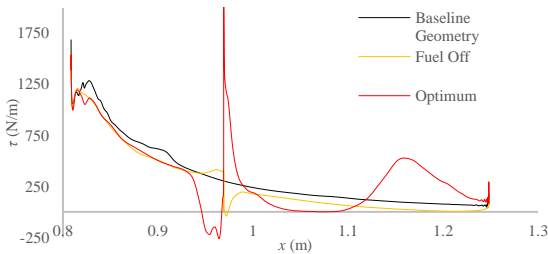

Figure 12. Surface pressure distributions.

Figure 13. Shear stress distributions.

Discussion

The scheme envisaged is effectively a combined-cycle scramjet rocket, or ejector scramjet. Whilst thrust is augmented substantially, specific impulse falls as the liquid oxygen injection rate increases. Similar after-burning schemes have been proposed and/or tested for rocket engines without any air-breathing. These include Supersonic After-Burning Rocket Engine (SABRE) [3] and Thrust Augmented Nozzle (TAN) [2, 7, 9]. TAN is a scheme introduced by GenCorp Aerojet in 2006 in which numerical simulations and physical testing were conducted on a thrust augmented nozzle, this incorporated hydrogen-oxygen combustion upstream of the rocket nozzle throat. It was found that a significant level of thrust augmentation was achieved, attributed to increased mass flow, inertia and energy in the nozzle resulting from the TAN injection propellants. Further, they were able to eliminate thrust penalties due to over expansion of the nozzle. TAN considered the injection of both fuel and oxidiser in order to augment thrust, this led to efficient combustion adjacent to the nozzle wall upstream of the TAN injectors. If a similar injection scheme were to be introduced in scramjet after-burning it would eliminate the limitations associated with supersonic mixing and the inherent effect on combustion.

Conclusions

As might be expected, a high correlation was found between thrust augmentation and injection pressure such that at higher injection pressures higher levels of thrust augmentation were attained. For the optimum injection configuration the total thrust acting upon the nozzle was found to increase by 300% in comparison to the baseline geometry. Observation of the force breakdown demonstrates that the thrust augmentation is due to the contribution of both inviscid forces acting upon the nozzle wall and increased momentum due to the fuel jet.

Comparison of the hydrogen mass fraction flowfields for the optimum injection configuration and baseline geometry indicate that less hydrogen remains at the nozzle outlet with the occurrence of injection, indicative of hydrogen combustion. The surface pressure acting on the nozzle wall was found to significantly increase in the region of the injection point and at the nozzle exit leading to a surface pressure increase of 125% when comparing the optimum injection configuration to the baseline geometry, this increase is one of the main sources of thrust augmentation. A similar occurrence was observed for the shear stress acting upon the nozzle wall. However, the increase was found to be less than 1% of the surface pressure increase and therefore was considered negligible. The complex phenomenon associated with the aerodynamics and chemical reactions in the scramjet nozzle introduced a scenario where an optimum configuration requires a fine balance between the parameters that are investigated in this paper.

Future work will include an investigation into the enhancement of mixing and combustion through improved turbulence, reaction and diffusivity modelling. This will be followed by a design optimisation through surrogate-assisted evolutionary algorithms focusing on minimising the energy associated with fuel injection whilst maximising the thrust increase due to combustion. Finally an alternative fuel injection configuration will be investigated *i.e.,* strut injector.

References

[1] Boyce, R. R., Tirtey, S. C., Brown, L., Creagh, M., and Ogawa, H., SCRAMSPACE: Scramjet-based Access-to-Space Systems, in *AIAA Paper 2011-2297*, 2011.

[2] Bulman, M., Thrust Augmented Nozzle (TAN): the New Paradigm for Booster Rockets, in *AIAA Paper 2006-4371*, 2006.

[3] Dorrington, G.E., Rationale for Supersonic Afterburning Rocket Engines, *Journal of Spacecraft*, **40**, 2002, 301-303.

[4] Drummond, J.P., Carpenter, M.H., and Riggins, D.W., *Progress in Astronautics and Aeronautics*, Sunset Books, 1991.

[5] Drummond, J.P., Diskin, G.S., and Cutler, A.D., *Technologies for Propelled Hypersonic Flight*, Scientific and Technical Aerospace Reports, 2006.

[6] Evans, J. S., and Schexnayder, Jr., C. J., Influence of Chemical Kinetics and Unmixedness on Burning in Supersonic Hydrogen Flames, *AIAA Journal*, **18**, 1980, 188-193.

[7] Ferrante, F.A. and Chen F.F., Thermal Design and Analysis of the Thrust Augmented Nozzle (TAN) Injector, *AIAA Paper 2006-4541,* 2006.

[8] Ferri, A., Moretti, G., and Slutsky, S., Mixing Processes in Supersonic Combustion, *Journal of the Society for Industrial and Applied Mathematics*, **13**, 1965, 229-258.

[9] Forde, S., Bulman, M. and Neill, T., Thrust augmentation nozzle (TAN) concept for rocket engine booster applications, *Acta Astronautica,* **59**, 2006, 271-277.

[10] Ogawa, H. and Boyce, R. R., Nozzle Design Optimisation for Axisymmetric Scramjets by Using Surrogate-Assisted Evolutionary Algorithms, *Journal of Propulsion and Power*, **28**, 2012, 1324-1338